RESEARCH ARTICLE

Controlled atomization using a twin-fluid swirl atomizer

J. Karnawat · A. Kushari

Abstract This paper presents the results of an experimental study of a twin-fluid internally mixed swirl atomizer. In this type of injectors, atomization is attained by injecting a small amount of air (i.e. of the order of less than 16% of the mass flow rate of liquid) into a liquid stream within the injector and the two-phase air liquid mixture is passed through a swirling passage to impart a swirling motion to the flow. Since most of the energy for atomization is supplied to the liquid by the atomizing air, a significantly small pressure drop can produce very fine spray with a small amount of atomizing air. At low values of air–liquid mass ratio (ALR), the appreciable tangential component of velocity with respect to the axial velocity provides a hollow cone spray structure, which turns into a solid cone spray with the increase in axial momentum, through either an increase in ALR or the liquid supply pressure. The results presented in this paper suggest that the investigated injector could be used to control the flow rate and spray characteristics (e.g. spray cone angle, spray solidity, breaking distance, and the droplet diameter) independent of each other by simultaneously varying the supply pressure of the liquid and the atomizing air flow rate. The controlled atomization studied in this paper for a twin-fluid internally mixed swirl atomizer makes it attractive to be used for various commercial applications as the atomizer is capable of providing various spray characteristics depending upon the application requirement.

J. Karnawat · A. Kushari (✉)
Department of Aerospace Engineering,
Indian Institute of Technology, Kanpur, India
e-mail: akushari@iitk.ac.in

Nomenclature

ALR	ratio of mass flow rates of the air to that of the liquid
D_b	spray break-up distance/breaking distance
$D_{orifice}$	orifice diameter
SMD	Sauter's Mean Diameter

1 Introduction

The process of breaking or atomization of the liquid fuel into tiny droplets in the form of a fine spray plays a vital role in various industrial and propulsion applications. The droplets provide a larger surface area than the liquid itself, thus, reducing the liquid vaporization time, which results in better mixing and increases the time available for complete combustion in liquid fueled combustion systems (Lefevbre 1983). The influence of spray quality on combustion/ignition performance and efficiency is well depicted in various works of Lefevbre, e.g., Lefevbre (1985), Rink and Lefevbre (1987), and Reeves and Lefevbre (1986). Typical issues pertaining to spray combustion are the non-symmetrical spray flames and the hot-streaks that can cause serious damage to the combustion liner and can severely effect the combustor exit temperature distribution. These issues are highly related to the spray pattern provided by a particular spray device as discussed by Chigier (1993). Thus, significant improvements in the performance of the liquid fueled combustors can be achieved by having the ability to control the spray characteristics and spray structure.

Various spraying devices operating on different principles and varied geometry have been developed

with time signifying the importance and high dependence of spray characteristics on both the above-mentioned factors. Detailed descriptions of such devices can be found in Giffen and Muraszew (1953), Lefevbre (1983, 1989), and Bayvel and Orzechowski (1993). This paper describes a method of obtaining controlled spray in terms of spray cone angle, spray solidity, breakup length factor as well as the droplet size from a novel internally mixed, twin fluid swirl atomizer, which makes use of a combination of the working principles of a pressure swirl and an air assisted atomizer.

In a simple pressure swirl atomizer (Giffen and Muraszew 1953; Lefevbre 1983, 1989; Bayvel and Orzechowski 1993; Ramamurthi and Tharakan 1995, 1998), swirling motion is imparted to the liquid inside the atomizer by passing it through a swirling chamber, which results in a tangential velocity component in the flow. This component results in a hollow and thin liquid cone formation once the liquid comes out of the orifice of the atomizer. In such atomizers, the atomization properties depend solely on the kinetic energy of the liquid at the exit of the atomizer, and, thus large pressure difference has to be maintained across the atomizer for quality atomization. Also, such atomizers cannot be used for applications that require solid cone sprays.

Lately, air-assisted atomizers are gaining popularity because of the controllability over the atomization process and the improved quality of atomization provided by them (Mullinger and Chigier 1974; Biswas 1982; Roesler and Lefevbre 1989; Chin 1995; Levy and Lubarsky 1996; Kushari et. al. 2001; Lee et. al. 2002). In such atomizers, a low flow rate of marginally pressurized air is impinged upon the liquid, a short distance from the injector's exit. It is believed that two effects induce atomization in such an injector. First, as both the liquid and the air share the same flow passage in the injector, the liquid is restricted to a smaller available flow area. The reduction in flow area accelerates the liquid thus increasing its kinetic energy, which induces fine atomization. Second, the relative motion between the air and the liquid phases produces shear force at their interface. This force strips liquid droplets from the liquid filaments inducing atomization. The potential advantage of such an injector is choking of the two-phase flow as it passes through the injector, due to the low sonic velocity of the two-phase liquid mixture (Biswas 1982). Therefore, the liquid fuel flow rate is relatively insensitive to variations in combustion chamber pressure and thus the fuel flow rate is not likely to respond to combustor disturbances reducing the chances of coupling of combustor pressure and fuel

flow oscillations. The positive aspect of the internally mixed air assisted atomizer is that its atomization characteristics can be controlled (Kushari et. al. 2001; Lee et al. 2002). This is possible as the atomization characteristics of the evolving spray can be varied in such a spray device by controlling air–liquid mass ratio (ALR) and liquid supply pressure.

It should be pointed out that some applications of liquid atomization require formation of hollow cone sprays due to their large coverage areas. But, some applications require solid cone sprays, which allows for local droplet injection. However, most of the commercial atomizers can provide either a hollow cone spray (pressure swirl atomizers) or a solid cone spray (air-assisted atomizers) but not both. This restricts the atomizers to be application-specific. It is envisaged that an atomizer that can provide both the hollow cone spray and the solid cone spray can find wider applications and hence, an effort was made to develop such an atomizer. The atomizer discussed in this study is capable of providing different spray characteristics at same liquid flow rate by varying liquid supply pressure and ALR. In this paper, the controllability of the spray in terms of cone angle, solidity, breaking distance, and droplet size were studied featuring this atomizer's capability of being an efficient spray device for a wide range of applications with different requirements in terms of spray properties or structure.

2 Experimental procedure

2.1 Injector design

The design of the atomizer discussed in this study is an enhanced version of a conventional pressure swirl atomizer modified to create a two-phase swirling flow by adding a small amount of air into the liquid. As the increase in the kinetic energy of the liquid in this atomizer is not only the function of the liquid supply pressure but also is a function of the amount of atomizing air, a good quality spray can be achieved with much less pressure drop across the atomizer. Two effects, the swirling effect and the axial momentum of the fluid, govern the spray pattern obtained through the atomizer. At low ALR, the swirling effect dominates resulting in a hollow cone spray structure. At high ALR, as the amount of atomizing air increases, the axial momentum component, which increases due to decrease in the liquid flow area, dominates resulting in a solid cone spray. At medium ALR, a pattern in variation of solidity varying from hollow structure to a perfectly solid cone structure is observed at varying

cone angles depending on the flow conditions maintained. Detailed description of the performance of the atomizer is presented later.

The cross-sectional view of the atomizer discussed in this paper is shown in Fig. 1. The liquid is supplied to the atomizer from the liquid inlet port of 6 mm in diameter. A small amount of air is introduced into the liquid stream through six radial holes, each of 0.8 mm in diameter, on the circular wall of the tube in which the liquid flows. Before interacting with the liquid, the air is allowed to settle in the settling chamber. This chamber ascertains the uniform distribution of air through the holes in the circular tube. The air coming out of the air inlet holes interacts with the liquid and creates a two-phase air liquid mixture, which then flows through the helical passage with a double threaded acme screw element fitting (acme thread of 1.82 mm^2 cross-section). This passage imparts the tangential component to the flow velocity. The rotating flow then passes through a swirling chamber (of a conical shape of 63°). This swirling two-phase flow finally comes out of the orifice (of 1 mm in diameter) of the atomizer at high velocity and the spray characteristics are obtained depending on the ALR and the other flow conditions maintained.

2.2 Experimental set up and methods

Figure 2 shows the schematic of the experimental set-up used for this study. For the purpose of liquid supply to the atomizer, the liquid was first stored in a cast iron vessel. High-pressure air was introduced to this vessel to drive the liquid through the pressure regulating valve, a metering valve and a flow meter to the atomizer at the required pressure conditions. The liquid injection pressure was measured using a pressure gage and could be varied using the regulating valve. The flow rate of the atomizing air was controlled and

measured using the air pressure regulating valve and the calibrated rotameter, respectively. For the sake of corrections in density variation, the supply pressure of the atomizing air was closely monitored using a pressure gage. The required variation in the air supply pressure to achieve the desired operating condition was also monitored and has been discussed along with the results.

In the present study detailed laser flow visualization (Karnawat and Kushari 2005) was carried out to understand the process of atomization for the atomizer being discussed. The spray produced from the atomizer was illuminated using a 25 mW He–Ne laser source of 632 nm wavelength. The laser beam was converted into a 1 mm thick sheet, by using a cylindrical lens. The laser sheet was passed through the centerline of the spray. A pixelfly® CCD camera was focused perpendicularly on the laser sheet and the spray images were captured in the computer to which the CCD camera was interfaced. Suitable exposure time (1 ms) was maintained to visualize the cone shape and the structure of the spray at varying ALR values (ranging from 0.001 to 0.16) for different liquid supply pressure (ranging from 207 to 552 kPa) conditions. Images obtained using the above mentioned procedures were analyzed for the spray characteristics such as cone angle, solidity and breaking distance using an image analysis code in MATLAB®.

The spray was required to be separated from the electronic noise (due to CCD device) and the background. In order to filter out the electronic noise, a sample snap (keeping the lens of the camera covered) was captured. This image was then subtracted from the spray images in order to deduct the effect of the electronic components. To filter the background optical noise, an image, containing only the background (keeping the spray off), was taken and the pixel wise intensity distribution was estimated. Once the spray

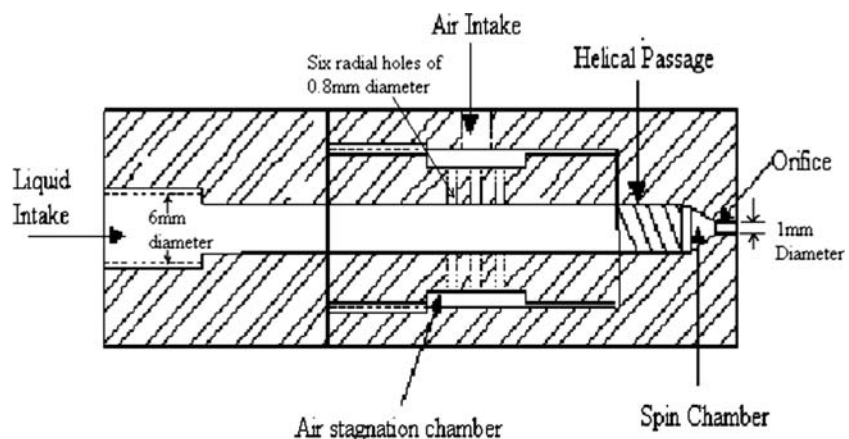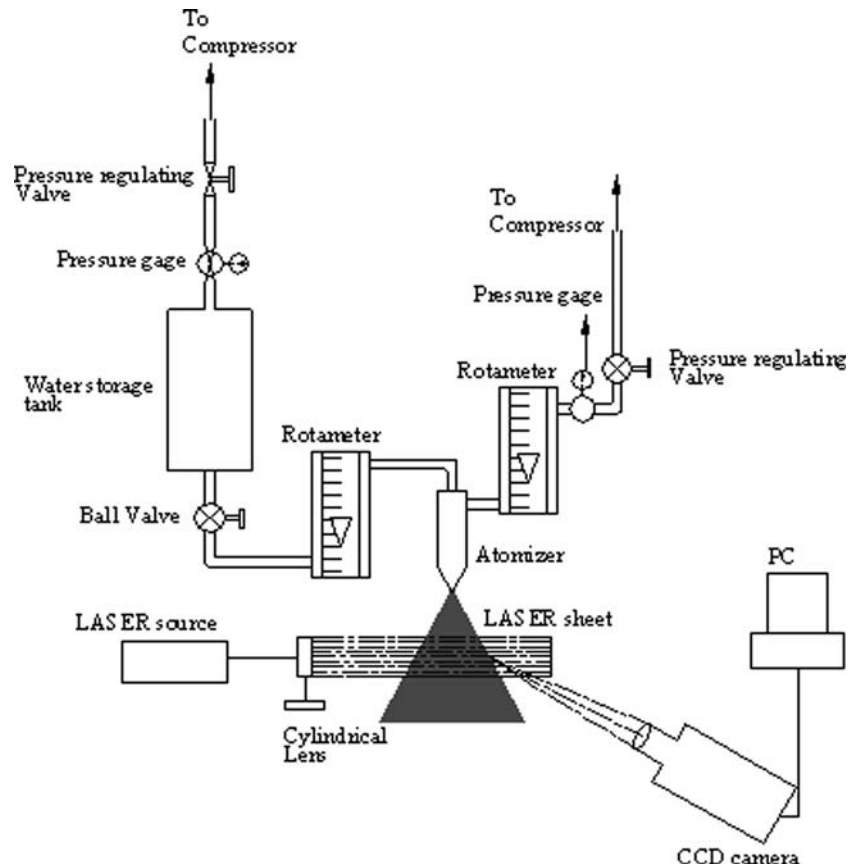**Fig. 1** Schematic of the twin-fluid internally mixed swirl atomizer

**Fig. 2** Schematic of the experimental setup

was turned on, the zone containing the spray got brighter than the background resulting in an increase in the corresponding pixel intensities in the image matrix. Thus, a pixel, in an image containing the spray, with an intensity value higher than the corresponding values in the image containing solely the background was considered to be the one representing the spray. The minimum intensity value for such pixels, representing the spray in an image, was then taken as the critical value for separating the spray in an image. For the present study the threshold pixel intensity to separate the spray from the surroundings was estimated to be equal to 60, for the digitized image in the scale of 100.

Figure 3a shows a representative grayscale image of spray produced by the atomizer. The grayscale images were processed further to estimate the spray angle, spray solidity, and the breaking distance. Once the spray region was identified using the procedure mentioned in the previous paragraph, the solid region of the spray was detected and was marked by two surfaces, i.e., the outer surface and the inner surface, as shown in Fig. 3c. The region between these two surfaces was the solid portion of the spray in which the liquid is enclosed. These surfaces were traced to a

vertical distance up to which the liquid column is continuous. The vertical distance below the injector orifice after which the cohesive liquid sheet disintegrates into ligaments has been defined as the breaking distance (D_b) in this study as shown in Fig. 3b. The average angle that the left outer surface made with the vertical reference line was termed as Angle 1 and the average angle for the right outer surface was termed as Angle 2 (see Fig. 3c). The left and right outer surfaces of the spray were analyzed separately for the cone angle measurement. These surfaces were divided in small segments containing 10 pixels each, as shown in Fig. 3a. The angle between each segment and the vertical reference line was estimated. The average of all these angles made by the small segments for left outer surface was termed as Angle 1 and for right surface was termed as Angle 2. The angle for the spray cone was then defined as the sum of Angles 1 and 2. Overlapping bins were used in this study to have a continuous representation of the spray surface. The spray was digitized into bins till the breakup distance was reached. The criterion for estimation of breaking distance has been explained later in the paper. The above mentioned image extraction procedure was repeated for ten consecutive images taken under the

Fig. 3 Schematic of step-wise surface extraction of the spray
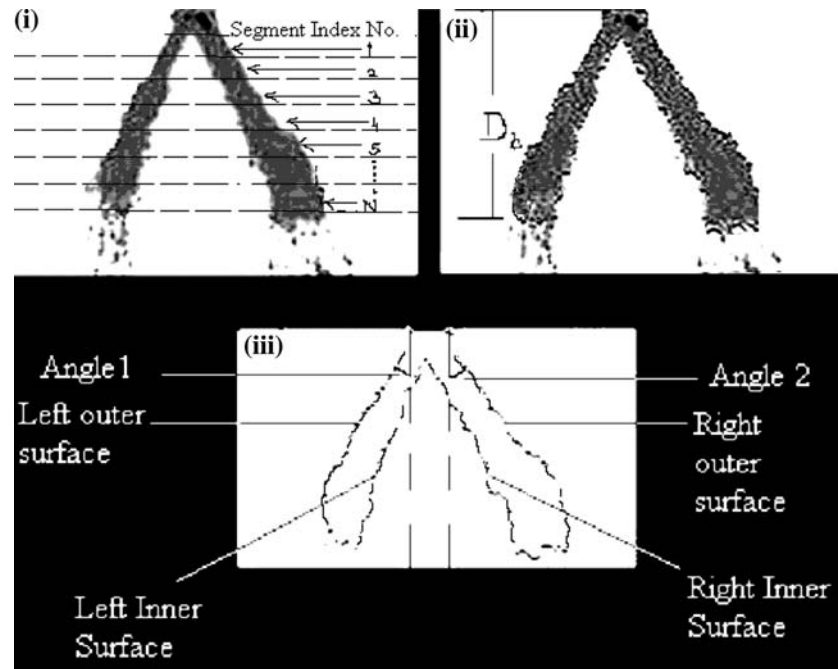
same ALR condition and the average value of all these images was considered as the cone angle for that operating condition.

The Spray solidity for this study was defined as the area of the spray region enclosed by liquid to the total area enclosed by the spray cone. The number of pixels enclosed in a defined region was taken as the measure of the area of that region. Thus, the solidity was measured as the ratio of the number of pixels under the outer surface with an intensity value greater than the critical value for the spray representation, i.e., 60, to the total number of pixels inside the outer surface of the spray. The solidity was estimated for the continuous liquid sheet before the sheet breakup. The value of solidity of the spray for a particular condition is obtained by estimating the average solidity for ten consecutive images.

As stated earlier, the distance from the injector exit at which the liquid sheet is shattered has been referred to as the breaking distance (D_b) for this study. In order to estimate the breaking distance, a particular pixel on the outer surface (with a unique row and column number in the intensity matrix of the original grayscale image) was considered. If the next five pixels on the outer surface, succeeding the pixel under consideration, continuously represent the next five row numbers (succeeding the row number corresponding to the pixel on the outer surface under consideration in the original image), the surface was then considered to be continuous and the breakage of liquid sheet did not occur. In case of a discontinuity, breakage was assumed

to have occurred. This procedure was repeated for all the pixels on the outer surface starting with the one with the lowest row value till the discontinuity is traced. The pixel location on the outer surface where breakage has occurred was then converted to the distance value by using proper pixel calibration. In this study, 37 pixels in a sample image represented 1 mm of distance. This process was repeated for several consecutive images and the average breaking distance was estimated.

An Ensemble Particle Concentration and Sizing apparatus (EPCS, Insitec/Malvern®, Worcestershire, UK) was used to measure the average droplet diameter of the spray. The operating principle of this apparatus is based on low angle laser light scattering. The dynamic measurement range for this system was between 0.5 and 1,000 μm. To determine droplet diameter from the input signals, EPCS uses a computer program (RTSizer, Insitec/Malvern®, Worcestershire, UK), which is based on the Mie theory of light-particle interactions. The instrument uses a 5 mW/670 nm diode laser with a beam diameter of 10 mm. The accuracy of the instrument was ±3% of full scale (specified by the manufacturer) and it could measure the size distribution of sprays with obscurations up to 95%. The measurement rate of equipment was one measurement every 400 μs. Measurements were taken along the centerline of the spray cone at a distance of 0.0762 m, i.e., 3 in. below the exit of the atomizer. Sauter Mean Diameter (SMD) was used as a meaningful quantity to represent the average of droplet

diameter. SMD represents an average droplet diameter with the same volume to surface area ratio as that of the entire spray. It should be noted that for fuel combustion applications, emphasizes is given to the use of this average diameter criteria, since it is least susceptible to a large spread in the droplet diameter distribution.

In the present study, the liquid supply pressure was kept constant and the air flow rate through the atomizer was varied over a range to obtain the variation in ALR. The spray structure parameters, i.e., spray cone angles, spray solidity, and breakup length were estimated using the procedure mentioned in the previous paragraphs. The liquid flow rate corresponding to a particular air flow rate (i.e., ALR) was measured using a calibrated rotameter. The liquid supply pressure was then varied and the entire procedure was repeated for different values of liquid supply pressure and a performance map was obtained. The spray structure corresponding to a range of liquid supply pressures (i.e. 207–552 kPa) and ALR (0.001–0.16) were studied. The results are presented in the next section. The corresponding change in the air supply pressure ranged between 207 and 620.5 kPa.

3 Results and discussion

In order to characterize the spray produced by the novel atomizer, an experimental study of the injector was carried out. The experimental investigation included study of spray structure (in terms of cone angle and solidity), breaking distance as well as the average droplet diameter that can be obtained from the device along with their dependence on the control parameters.

Ideally one would like to control the spray structure independent of the liquid flow rate so that the fuel/air ratio in the combustor is a constant and the variations in chemical effects can be ignored. However, the liquid flow rate through a pressure-swirl atomizer is a function of the liquid supply pressure (Ramamurthi and Tharakan 1995) and that through an internally mixed air-assisted atomizer a function of both the liquid supply pressure as well as the ALR (Kushari et al. 2001). Therefore, the effect of the variations in ALR as well as the liquid supply pressure on the liquid flow rate through the investigated atomizer were studied and the results are plotted in Fig. 4a, which depicts the variation in liquid flow rate with ALR for different liquid supply pressures. The required variation in the air supply pressure, non-dimensionalized by the liquid supply pressure, that will provide the desired variations in the operating parameters are plotted in Fig. 4b. It should be pointed out that the higher limit of the operating ALR for a particular liquid supply pressure corresponds to the condition beyond which both the liquid flow as well as the air flow become unsteady, producing an unsteady spray that is not desirable for any particle application of the device. This unsteadiness can be attributed to the large kinetic energy of the liquid flow at high ALR, caused by increased air induced blockage, leading to shear rapture of the air bubbles as well as loss of continuity in both the phases (i.e. gas and liquid) at high ALR. The data in Fig. 4a show that the maximum operating ALR for a constant supply pressure decreases with an increase in the liquid supply pressure, which points to the fact that the increase in liquid kinetic energy due to increased pressure difference across the atomizer causes an early transition to unsteady flow.
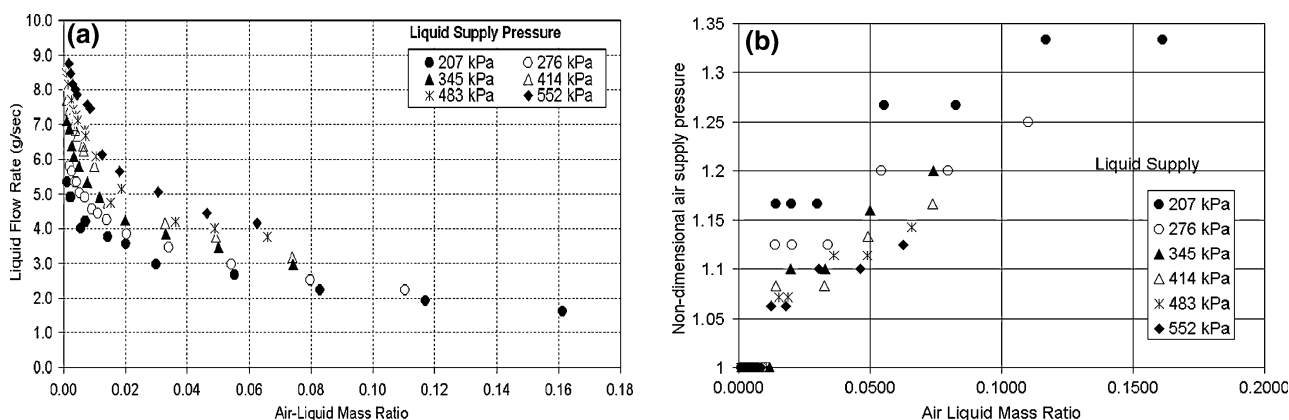

Fig. 4 a Liquid flow rate versus ALR relationship for different liquid supply pressures; **b** variation in air supply pressure (non-dimensionalized by liquid supply pressure) to accomplish the required ALR variation

The data in Fig. 4a also show a monotonic decrease in the liquid flow rate with an increase in ALR for a given supply pressure. This indicates a decrease in the discharge coefficient of the atomizer with an increase in ALR at the same liquid supply pressure. The reason for this decrease in the liquid flow rate can be attributed to the fact that with the increase in the area occupied by the air due to the increase in its flow rate with ALR, the area available for liquid flow decreases and is thus reducing the liquid flow rate. Furthermore, the pressure inside the atomizer increases as the air flow rate and the corresponding air supply pressure increases with the increase in the ALR, as shown in Fig. 4b, thus, further reducing the liquid flow rate through the injector. It can also be seen that the liquid flow rate increases with the liquid supply pressure for a constant value of ALR, which is due to the increased liquid head. The data is Fig. 4b shows that the air supply pressure needed to be increased beyond the liquid supply pressure in order to force the desired amount of air into the liquid stream. However, the maximum air supply pressure was only 33% higher than the corresponding liquid supply pressure for an ALR value of 0.16.

The two components that play vital roles in determining the spray structure in the presented atomizer are the axial momentum and the tangential or the swirling effect. The axial momentum of the flow controls the solidity pattern of the spray where as the tangential momentum controls the radial sweep of the cone or the cone angle. Therefore, when the tangential momentum component dominates the flow, a hollow cone spray structure is obtained owing to high centripetal acceleration. This corresponds to a situation having a low value of ALR. At a low ALR value of the order of 10^{-3}, a hollow cone structure with relatively large cone angle is obtained as shown in Fig. 5a. At high ALR conditions of 0.16 a solid cone shape was observed as seen in Fig. 5b.

One interesting feature of the picture presented in Fig. 5a is that a fully developed air core is present in the flow causing the formation of a fully developed hollow cone spray. For conventional pressure-swirl atomizers such flow structure is not possible at such a low supply pressure. Instead a tulip shaped spray will be observed as discussed by Ramamurthi and Tharakan (1995, 1998). They have suggested that the development of a fully developed air core leading to the formation of a hollow cone spray at higher supply pressure in swirl atomizers is due to the increased axial velocity prior to the swirler, causing an increase in the tangential velocity in the swirl chamber. Therefore, the formation of the hollow cone spray at such low pres-
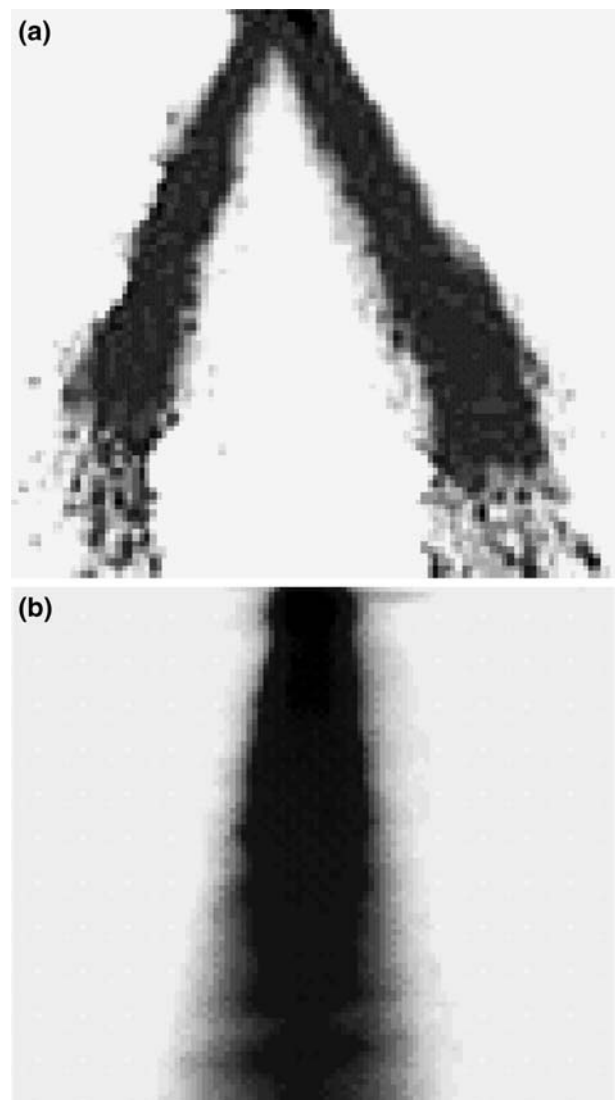

Fig. 5 Variation in spray structure with change in ALR at a liquid supply pressure of 207 KPa; **a** ALR = 0.001, **b** ALR = 0.16

sure is the indication of the assistance received by the liquid due to its interaction with air, resulting in an increase in the total forces acting on the liquid. It should be pointed out that the air pressure corresponding to such low ALR conditions, giving rise to fully developed air cone and a hollow cone spray, are equal to the liquid supply pressure as seen in Fig. 4b.

The variation in the spray solidity with ALR for different liquid supply pressures is shown in Fig. 6. The data in Fig. 6 show a monotonic increase in spray solidity with an increase in ALR for a given liquid supply pressure. With the increase in the ALR, the mass flow rate of the liquid decreases as seen in Fig. 4 and discussed in the previous paragraphs. The air in the outer annular starts pushing the liquid more and more in the inner core with the increase in the amount of

Fig. 6 Solidity versus ALR variation for different liquid supply pressures
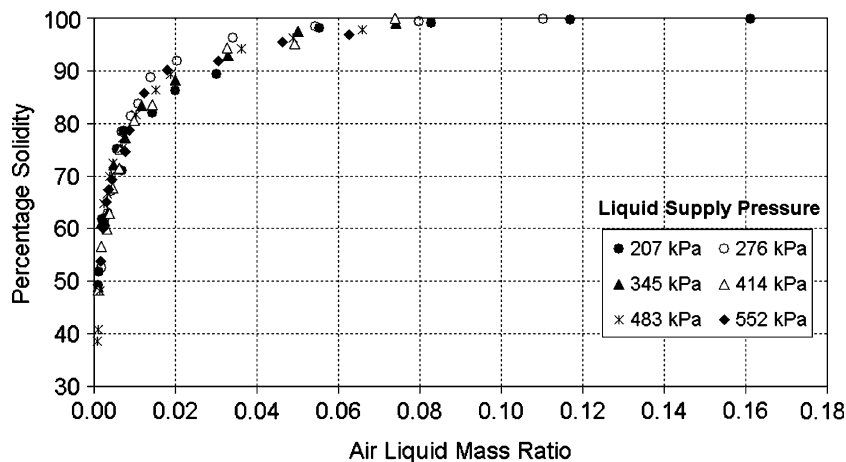
atomizing air impinged in the atomizer. This squeezing of the liquid core results in an increase of the axial velocity of the liquid due to the reduced liquid flow area. The resulting increase in axial momentum of the liquid overpowers the centrifugal effects induced by the swirling motion resulting in a solid cone. At medium ALR, a pattern in variation of solidity varying from hollow structure to a perfectly solid cone structure was observed at varying cone angles depending on the flow conditions maintained. The increase in flow momentum due to the rise in liquid supply pressure is insignificant with respect to the effect of the interaction between the liquid and air. Therefore, for a given value of ALR, the spray solidity is almost independent of the supply pressure, with a marginal increase in solidity with increasing pressure as seen in Fig. 6.

For a constant liquid supply pressure, a decrease in the spray cone angle is observed with an increase in ALR as seen in Fig. 7. Air being lighter than water, due to the centrifugal acceleration (imparted by the swirling motion), tends to flow toward the periphery of the two-phase mixture. This leads to the establishment

of an annular flow. When the air–liquid flow becomes annular, the air flows in an outer annulus over the liquid core. With the increase in ALR, the air in the outer annular starts pushing the liquid in the inner core more and more, resulting in increasing the axial velocity of the liquid and, thus, restricting the radial spread of the liquid once it leaves the atomizer orifice. This effect results in the contraction of the cone angle of the spray. From the data presented in Fig. 7, it was also observed that for a low value of ALR, the cone angle increases with an increase of the liquid supply pressure. As discussed earlier, at low ALR values, when the interactive force between the phases is weak, the swirl can be effective in providing a tangential velocity component to the flow. Liquid at a higher supply pressure can be associated with higher energy, thus a higher tendency to spread outward (due to centrifugal effects) pushing the air surrounding it and, thus, higher is the cone angle. However, at higher values of ALR, the interactive forces between the air and liquid completely overwhelms the liquid pressure forces, thus, providing such a high axial momentum to

Fig. 7 Spray cone angle versus ALR variation for different liquid supply pressures
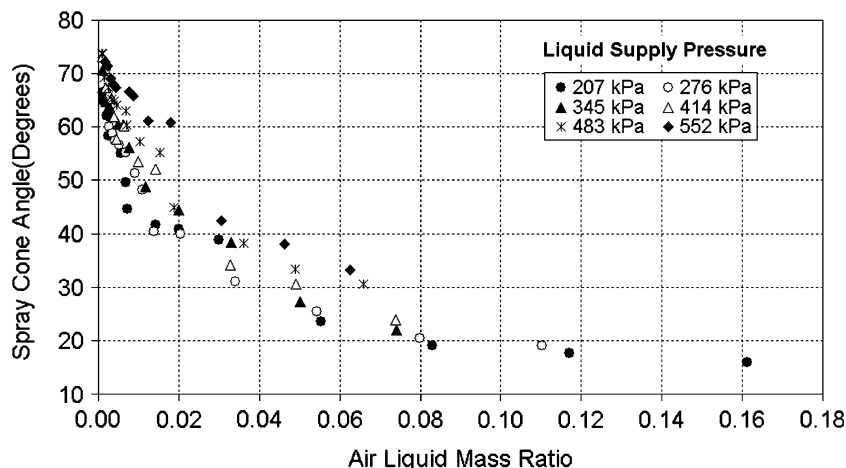
the flow that the swirl effect is almost negligible. And hence, at such values of ALR, the spray acquires a solid cone shape and the spray angle is independent of liquid supply pressure as seen in Fig. 7. It should be noted that the maximum achievable spray angle is limited to about 70° in this case. But by increasing the degree of swirl through some design modification, which is beyond the scope of the present study, this angle can further be increased.

The variation of spray solidity with changing spray cone angle is presented in Fig. 8 for different liquid supply pressures. It should be noted that the high solidity and low cone angle corresponds to high values of ALR and high cone angle, i.e., low solidity, corresponds to low values of ALR. Considering solidity to be primarily governed by the axial flow momentum and the cone angle by tangential flow momentum, it can be seen in Fig. 8 that the solidity increases monotonically with a decrease in the cone angle for a given liquid supply pressure, which corresponds to the effect of increased liquid acceleration due to increasing ALR.

It can also be seen that for a fixed cone angle, the solidity increases with an increase in liquid supply pressure. On the other had, an increase in supply pressure for a constant value of solidity leads to an increase in cone angle owing to the increase in tangential momentum corresponding to the increase in overall energy.

A performance map for the investigated injector vis-à-vis the spray solidity and liquid flow rate is presented in Fig. 9 for various liquid supply pressures. The data in Fig. 9 indicate that in contrast to the behavior exhibited by pressure atomizers, the investigated injector can atomize very small liquid flow rates into very fine sprays (as seen in the inserted pictures). This observation suggests that the investigated atomizer can be effectively used to obtain good atomization during engine start up and idling.

The performance map in Fig. 9 shows that varying the liquid supply pressure while keeping the liquid flow rate constant provides means for controlling the spray's solidity. This can be achieved by moving along a ver-

Fig. 8 Variation in spray solidity with respect to the spray cone angle for different liquid supply pressures
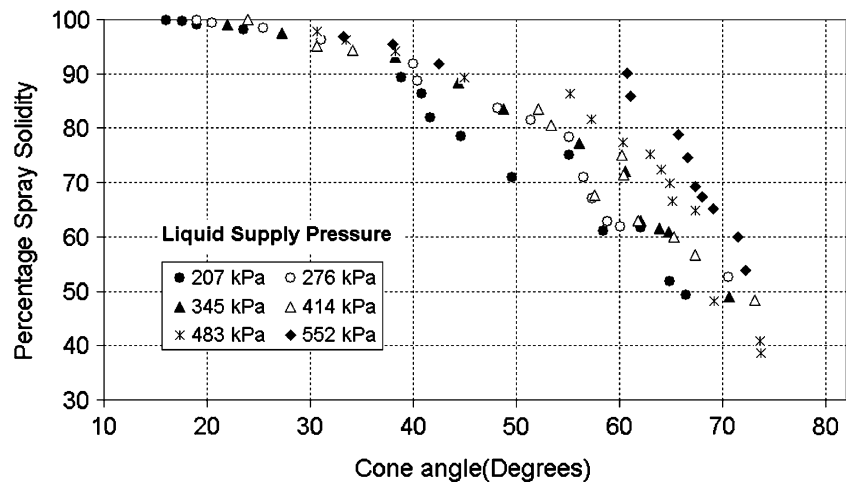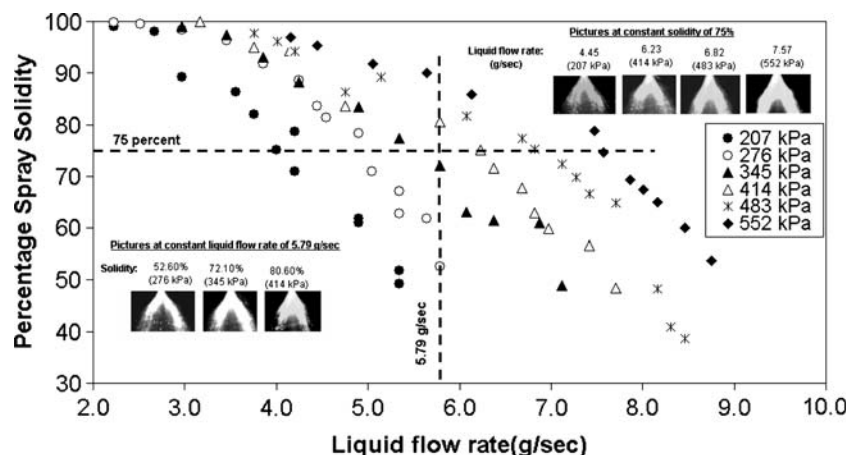

Fig. 9 Solidity versus liquid flow rate relationship for different liquid supply pressures. The inserted pictures represent various controlled spray conditions

tical line in Fig. 9. Similarly, changing the liquid supply pressure along the horizontal line in Fig. 9 provides means for changing the liquid flow rate while keeping the spray solidity constant. The inserted pictures in Fig. 9 demonstrate the spray solidity variation at constant liquid flow rate of 5.79 g/s and the liquid flow rate variation at constant solidity of 75% for different liquid supply pressures. The data in Fig. 9 show that in order to increase the liquid flow rate through the presented atomizer, the liquid supply pressure needs to be increased. However, that leads to a decrease in the spray solidity. Therefore, the ALR needs to be increased in order to compensate for this decrease in solidity. However, the required increase in pressure and ALR will lead to an overall increase in the total energy and momentum of the system, causing a spread in the cone angle of the spray.

Another performance map of the investigated atomizer depicting the variation in spray cone angle with the liquid flow rate is presented in Fig. 10. The data in Fig. 10 show that the spray cone angle can be maintained at a constant value and the liquid flow rate can be changed over a range by traversing along a horizontal line in the figure. The pictures inserted in the figure show that indeed the spray cone angle can be kept at 38° angle while the liquid flow rate can be varied from 2.97 to 4.55 g/s. The increase in the liquid flow rate for a constant cone angle can be accomplished by simultaneous increase in liquid supply pressure and ALR with a corresponding increase in the spray solidity. Similarly, by traversing along a vertical line, the spray cone angle can be varied while keeping the flow rate constant. The inserted pictures in Fig. 10 show that the spray cone angle can be changed from 53.4 to 70.6° for a constant flow rate of 5.79 g/s.

It should be noted that the required operating parameter, i.e., ALR, air supply pressure, and liquid

supply pressure variations for the data presented in Figs. 9 and 10 are in accordance to the data presented in Fig. 4a, b.

The variation of non-dimensional breaking distance (non-dimensionalized by the orifice diameter) with ALR for different liquid supply pressure can be seen in Fig. 11. In the fully developed spray under consideration, the breakup distance (D_b) depends solely on the kinetic energy of the liquid. As the ALR increases, the velocity of the liquid coming out of the injector increases (due to the squeezing effect caused by the atomizing air, as discussed before), thus, the magnitude of surface and frictional forces starts to increase due to the higher relative velocity of the fluid with respect to the ambient. In such a case, a higher amount of kinetic energy gets utilized in overwhelming these forces resulting in a decrease in the breakup distance. Therefore, the breaking distance decreases rapidly with an increase in ALR, as seen in Fig. 11. However, beyond a critical value of ALR, the liquid comes out of the atomizer in the shape of ligaments as slug or frothy two-phase flow is created inside the atomizer. Beyond that point, the breaking distance is independent of further increase in the kinetic energy as the liquid is already broken and primary atomization has started. In that domain a very dense spray is created at the exit of the atomizer and the image processing technique used in the present study finds it quite difficult to distinguish between the continuous liquid cone and the particles having sizes less than the pixel sizes. The data in Fig. 12 show that for a given supply pressure, the breaking distance increases with an increase in the liquid flow rate in a manner similar to that exhibited by conventional swirl atomizers (Ramamurthi and Tharakan 1995). But that can be kept constant by simultaneously varying the ALR, and thus a constant breaking distance can be maintained for different li-

Fig. 10 Spray cone angle versus liquid flow rate relationship for different liquid supply pressures. The inserted pictures represent various controlled spray conditions
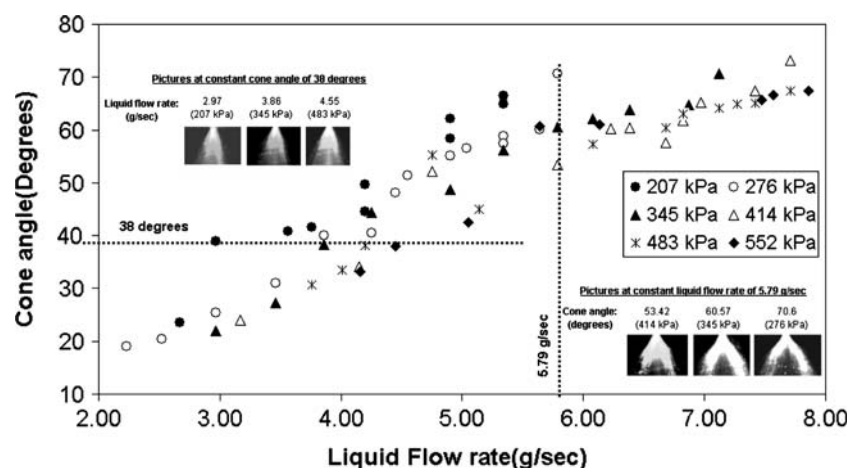
Fig. 11 Non-dimensional breaking distance versus ALR for different liquid supply pressures. The breaking distance is non-dimensionalized with respect to the orifice diameter
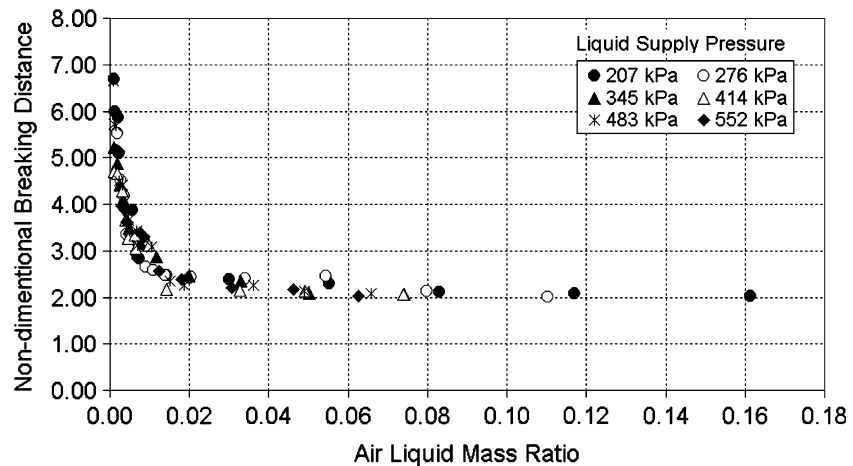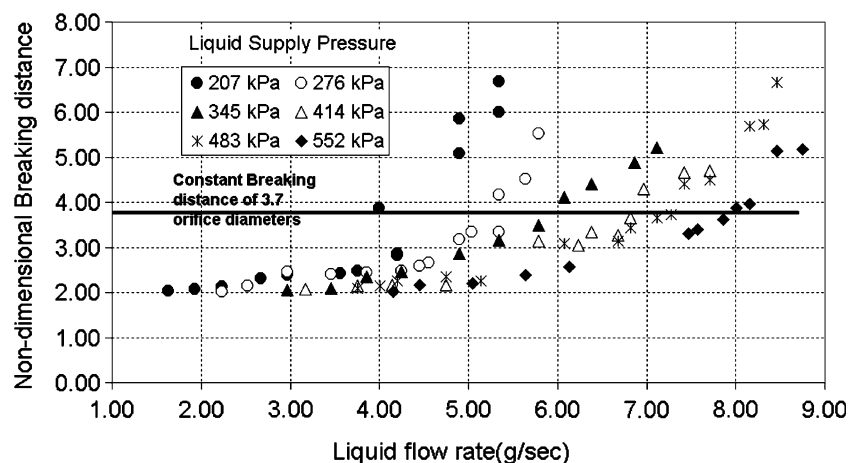

Fig. 12 Breaking distance versus liquid flow rate for different liquid supply pressures

quid flow rates, as exhibited by the horizontal line shown in Fig. 12. This property of the presented atomizer can be used by combustor designers to decide the location of the flame holding device without having to bother about the off-design variation in spray structure. However, it should be pointed out that a constant breaking distance may not guarantee constant flame holding, as the droplet size, spray cone angle and spray solidity all play significant roles in the final evaporation, mixing and combustion.

Perhaps the most important spray parameter related to the characteristics of the spray is the droplet size. It has been seen earlier (Kushari et al. 2001) that varying the ALR and the liquid supply pressure simultaneously can control the droplet size produced by an internally mixed air-assisted atomizer. In this study, the droplet size was measured for various operating conditions. The results are presented in Figs. 13 through 16.

The data presented in Fig. 13 show that for a constant liquid supply pressure, the SMD decreases with an increase in ALR. This can be attributed to the increase in the kinetic energy of the liquid due to its

interaction with the atomizing air as discussed earlier. First, the increase in the kinetic energy of the liquid helps in better atomization, thus, results in a lower mean droplet size of the spray. Second, the increase in airflow rate is accompanied by the increase in the air velocity and, thus, the shear force that it exerts upon the liquid. This increased shear force "strips" smaller droplets from the bulk liquid flow, resulting in improved atomization. The droplet size distributions for a liquid supply pressure of 207 kPa and ALR of 0.0013 and 0.083 are presented in Figs. 14a, b, respectively. The particle size distribution at a low ALR of 0.0013 (SMD of 113.81 μm), shown in Fig. 14a, depicts the presence of larger droplets compared to the case of higher ALR of 0.083 (SMD of 52.57 μm), shown in Fig. 14b, where the percentage of smaller size droplets have increased significantly, reflecting an improved atomization at higher ALR.

The data in Fig. 13 also show that for a constant ALR, SMD decreases with an increase in the liquid supply pressure. Liquid at a higher supply pressure can be associated with higher kinetic energy. This higher

Fig. 13 Variation of Sauter Mean Diameter (*SMD*) of the spray with ALR for different liquid supply pressures
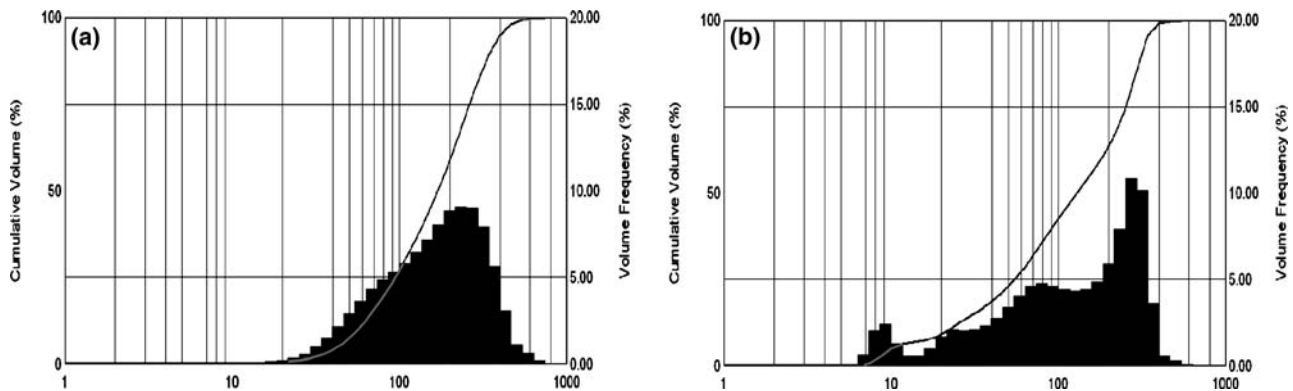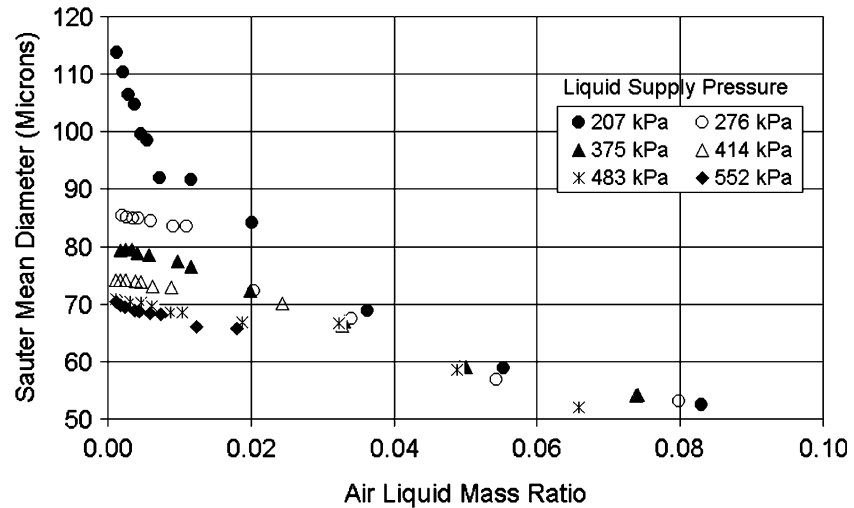

Fig. 14 Droplet size distributions for a constant liquid supply pressure of 207 kPa: **a** ALR = 0.0013, **b** ALR = 0.083

kinetic energy of the liquid results in better atomization of the liquid reducing the mean droplet size value with the increase in the liquid supply pressure. The particle size distributions for a constant ALR of 0.003 for different liquid supply pressures are shown in Fig. 15. The data show an increase in the fraction of smaller droplets in the expense of bigger droplets as the liquid supply pressure is increased. A corresponding variation in SMD from 104 μm for 207 kPa pressure to 69 μm for 552 kPa pressure was observed.

The variation in SMD with the liquid flow rate at different liquid supply pressures can be seen in Fig. 16. As in the case of other spray properties discussed earlier, the droplet size can also be changed in the present atomizer, independent of the liquid flow rate, by simultaneously varying the liquid supply pressure and ALR. The vertical line in Fig. 16 represents an SMD variation from 110 to 66 μm for a constant liquid flow rate of 5 g/s. The horizontal line in Fig. 16 represents a constant SMD of 70 μm for which the liquid flow rate was varied from 3 to 8.75 g/s.

An important observation regarding the behavior of the spray produced by the given atomizer is that beyond an ALR of around 0.02, the spray characteristics, i.e., spray solidity, cone angle, and breaking distance, show an asymptotic behavior. From the constant cone angle observation beyond the critical ALR value it can be inferred that in this region the increase in the kinetic energy of the liquid (because of an increase in velocity due to the reduction in liquid flow area) is mainly contributed to the increase in the axial component of the velocity of the liquid without affecting the tangential component value to a significant amount, thus, the effect on the spray cone angle (which depends mainly on the tangential component of the velocity) beyond the critical ALR value is negligible. The axial velocity of the flow can affect two characteristics of the spray, i.e., the spray solidity and the atomization characteristics. As the solidity value reaches a saturated state shortly beyond the critical ALR condition, the whole kinetic energy increase (with the increase in ALR) in this region contributes to the atomization of
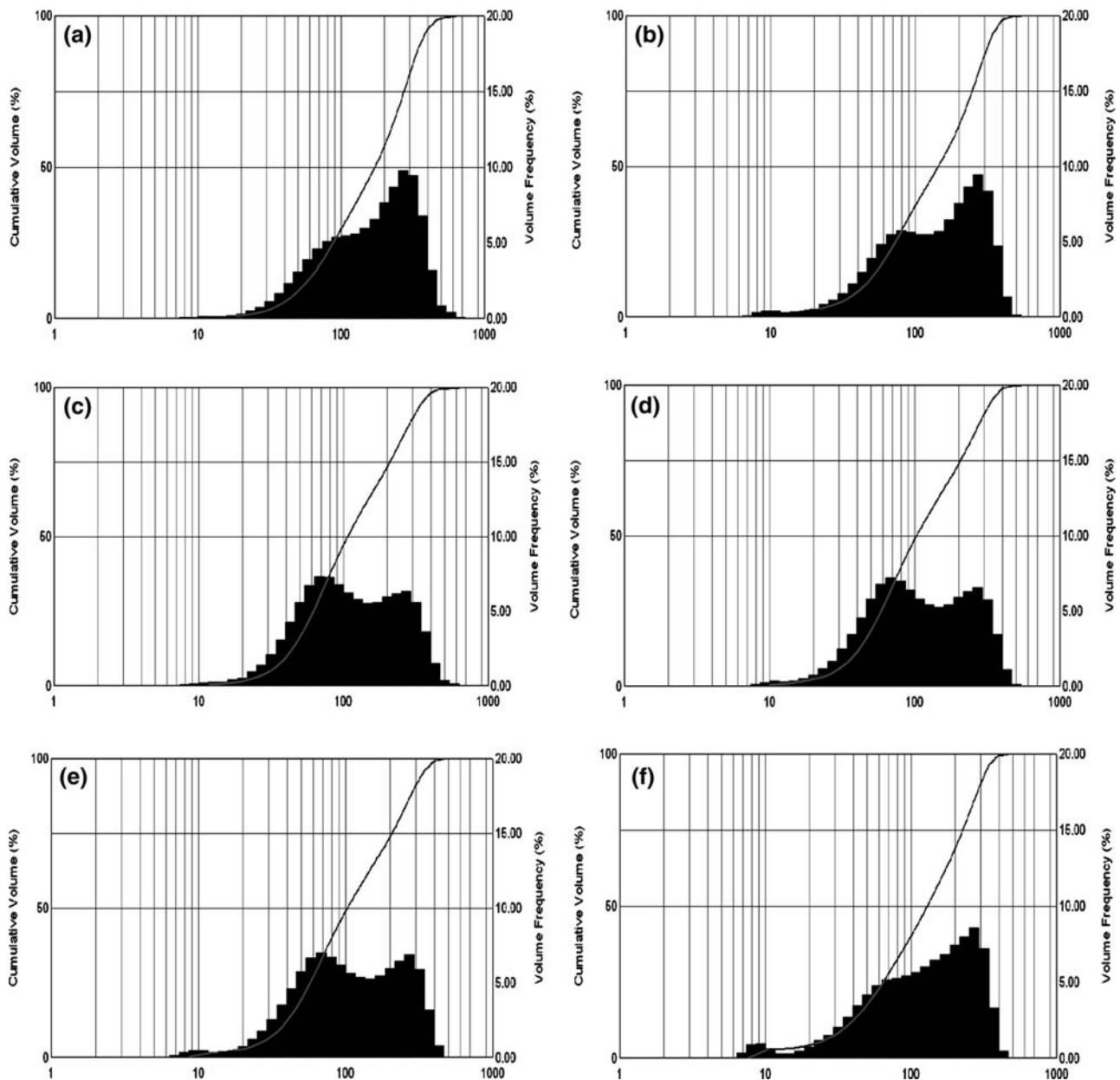
Fig. 15 Droplet size distribution for a constant ALR of 0.003 for: **a** 207 kPa, **b** 276 kPa, **c** 375 kPa, **d** 414 kPa, **e** 486 kPa, **f** 552 kPa

the liquid. Furthermore, the breaking distance too remains nearly a constant beyond the critical value. From this it can be inferred that beyond the ALR value of 0.02, most of the kinetic energy of the liquid is contributing in increasing the velocity of droplets formed during the atomization process resulting in negligible changes in the spray characteristics like cone angle and the breaking distance. It can be speculated that if the only change in spray characteristics beyond an ALR is an increasing droplet velocity, it will improve the quality of secondary atomization, resulting in marginal drop in the droplet diameter as seen in Fig. 13, while

the primary atomization process will be saturated beyond the critical ALR.

The formation of spray with varied cone angles and solidity ranging from a hollow cone to a perfectly solid cone with an efficient controllability over the breaking distance and droplet size, independent of the liquid flow rate, provides the atomizer discussed in this paper with extraordinary flexibility of being efficiently used for different applications. Particularly, the controllability of the spray structure is the feature that adds uniqueness to this novel atomizer design and can make it an effective spray device for the future.

Fig. 16 Variation of spray
SMD with the liquid flow rate
for different liquid supply
pressures
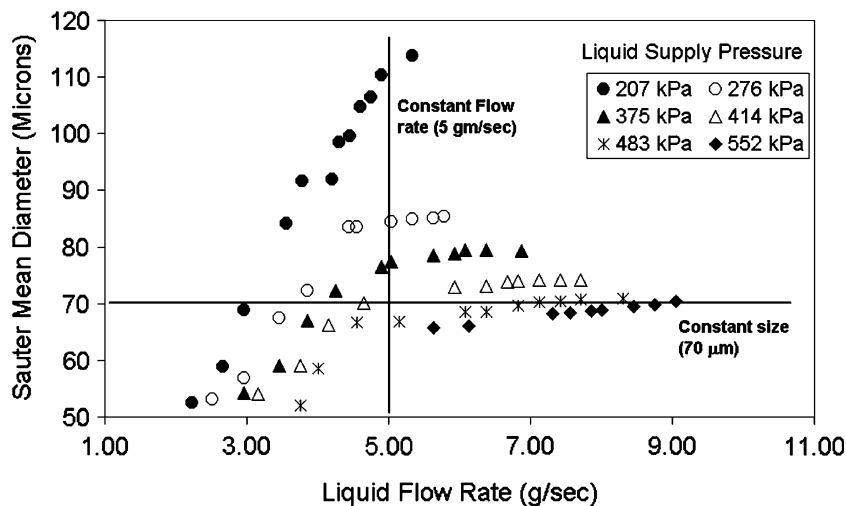
4 Conclusions

Although the atomizer studied in this paper combines
the principles of the swirl as well as internally mixed,
air assisted, twin fluid atomization; the mechanism of
atomization and the characteristics of the spray ob-
tained from it are distinctly different from both pres-
sure swirl and air assisted atomizers. It can be clearly
concluded from the study that this atomizer can be
effectively used to provide a wide range of spray pat-
terns in terms of spray cone angle, solidity and droplet
size of the spray by adjusting liquid supply pressure
and the ALR. Adjusting the factors mentioned above,
this atomizer could provide a spray pattern varying
from a very low solidity value to a solid cone at dif-
ferent spray cone angles depending upon the flow
conditions maintained. In the presented study, using
the same atomizer, a variation from 16 to 74° of the
spray cone angle was achieved. The spray solidity for
the range of operating conditions changed from 38.5 to
100%. These variations were achieved for a liquid flow
rate ranging between 2.23 and 7.86 g/s and the liquid
supply pressure variation of 207–552 kPa. The air
supply pressure was kept marginally higher than the
liquid supply pressure with the maximum operational
air supply pressure being 33% higher than the corre-
sponding liquid supply pressure at a large value of
ALR. The sheet breaking distance also changed be-
tween 6.68 times the orifice diameter to as low as 2.3
times the orifice diameter. The SMD of the spray
varied between 115 and 52.5 μm and a control over the
droplet size was achieved by simultaneously varying
the liquid supply pressure and the ALR.

This controlled spray pattern phenomena studied in
this paper for a novel twin-fluid, internally mixed, swirl
atomizer makes it efficient enough to be used for

various commercial applications. As the atomizer is
capable of giving sprays with varied properties and
structures, it is very flexible to be used for different
requirements depending upon the application.

References

Beyvel L, Orzechowski Z (1993) Liquid Atomization. Taylor and
Francis, Philadelphia, PA

Biswas MN (1982) Atomization in two-phase critical flows. In:
Proceedings of the 2nd International Conference on Liquid
Atomization and Sprays, pp 145–151

Chigier NA (1993) Spray science and technology, fluid
mechanics and heat transfer in sprays. ASME Fluid Eng Div
Publ FED 178:1–18

Chin JS (1995) Effervescent atomization and internal mixing air-
assisted atomization. Int J Turbo Jet Engines 12:119–127

Griffen E, Maraszew A (1953) The atomization of liquid fuels.
Chapman and Hall Ltd., London

Karnawat J, Kushari A (2005) Spray evolution in a twin-fluid
swirl atomizer. In proceedings ILASS—Asia, Seoul, Korea,
11–13 October 2005

Kushari A, Neumeier Y, Israeli O, Lubarsky E, Zinn BT (2001)
Internally mixed liquid injector for active control of
atomization process. AIAA J Propulsion Power 17(4):878–
882

Lee JY, Kushari A, Lubrasky E, Zinn BT, Rozenberg S, Levy Y
(2002) Control of combustion instabilities and emissions
using an internally mixed liquid atomizer with a vaporizer.
In: proceedings of AIAA 2002-0617, 40th aerospace sciences
meeting and exhibit. Reno, NV

Lefevbre AH (1983) Gas turbine combustion. Hemisphere
Publishing Corporation, Washington, DC

Lefevbre AH (1985) Fuel effects on gas turbine combus-
tion—ignition, stability and combustion efficiency. ASME J
Eng Gas Turbine Power 107:24–37

Lefevbre AH (1989) Atomization and spray. Hemishpere Pub-
lishing Corporation, New York

Levy Y, Lubarsky E (1996) Oscillating control spray for the
suppression of the low frequency combustion instabilities.
In: Proceedings of 36th Israel annual conference on aero-
space sciences, Haifa, Israel

Mullinger PJ, Chigier NA (1974) The design and performance of internal mixing multijet twin fluid atomizers. J Inst Fuels 47:251–261

Ramamurthi K, Tharakan TJ (1995) Experimental study of liquid sheets formed in coaxial swirl injectors. AIAA J Propulsion Power 11(6):1103–1109

Ramamurthi K, Tharakan TJ (1998) Flow transition in swirled liquid sheets. AIAA J 36(3):420–427

Reeves CM, Lefevbre AH (1986) Fuel effects on aircraft combustor emissions. ASME paper 86-GT-212

Rink KK, Lefevbre AH (1987) Pollutant formation in heterogeneous mixtures of fuel drops and air. AIAA J Propulsion Power 3(1):5–10

Roesler TC, Lefevbre AH (1989) Studies on aerated liquid atomization. Int J Turbo Jet Engines 6(3–4):221–230